ELSEVIER

Polymer 43 (2002) 4047-4054

polymer

www.elsevier.com/locate/polymer

Theoretical representation of shear and pressure influence on the phase separation behavior of PVME/PS mixture

Zhaoyan Sun[a,b,1], Jian Yang[a,2], Wei Jiang[a], Lijia An[a,*], Zhenhua Jiang[b], Zhongwen Wu[b]

[a]*State Key Laboratory of Polymer Physics and Chemistry, Changchun Institute of Applied Chemistry, Chinese Academy of Sciences, Changchun 130022, People's Republic of China*

[b]*Department of Chemistry, Research Center of Superior Engineering Plastics, Jilin University, Changchun 130023, People's Republic of China*

Received 22 May 2001; received in revised form 22 March 2002; accepted 26 March 2002

Abstract

In the framework of lattice fluid model, the Gibbs energy and equation of state are derived by introducing the energy (E_s) stored during flow for polymer blends under shear. From the calculation of the spinodal of poly(vinyl methyl ether) (PVME) and polystyrene (PS) mixtures, we have found the influence of E_s on equation of state in pure component is inappreciable, but it is appreciable in the mixture. However, the effect of E_s on phase separation behavior is extremely striking. In the calculation of spinodal for the PVME/PS system, a thin, long and banana miscibility gap generated by shear is seen beside the miscibility gap with lower critical solution temperature. Meanwhile, a binodal coalescence of upper and lower miscibility gaps is occurred. The three points of the three-phase equilibrium are forecasted. The shear rate dependence of cloud point temperature at a certain composition is discussed. The calculated results are acceptable compared with the experiment values obtained by Higgins et al. However, the maximum positive shift and the minimum negative shift of cloud point temperature guessed by Higgins are not obtained. Furthermore, the combining effects of pressure and shear on spinodal shift are predicted.

Keywords: Shear; Pressure; Polymer mixture

1. Introduction

The shear influence on phase behavior is very substantial for some polymer solutions and polymer mixtures. Different researchers [1–39] have made a lot of interesting work about the shear dependence of phase separation behavior because this phenomenon is of great importance to the practical process. Owing to the difficulty of experiment, there have been only a few reports [40,41] directly showing the shift of cloud point at a fixed shear rate. In these measurements, the shear-induced demixing and shear-induced mixing were observed by Higgins and co-workers [40,41] at a fixed composition and a constant shear rate for different temperature in the blend PVME/PS. Thermodynamically, Horst and Wolf [42–44] have dealt with the effects of shear rate on phase diagrams on the basis of Flory–Huggins [45–48] theory and calculated some phase diagrams for the model systems of polymer solutions and polymer mixtures. However, it is still difficult to understand the occurrence of lower critical solution temperatures (LCST) on the basis of the original FH theory because of the ignorance of free volume effects unless a particular dependence of the Flory–Huggins interaction parameter on temperature and composition is considered. In addition, the used combining rules [43,44,49] for the zero-shear viscosity and the steady-state shear compliance failed to describe the PVME/PS system in the above calculation [40]. According to the reasons mentioned earlier, the shear influence on phase separation behavior is introduced into the Sanchez–Lacombe lattice fluid model [50–52] (SLLF model) in this work because it is normally used to predict the equilibrium phase behaviors of polymer systems with LCST. Meanwhile, a valid combining rule [53] is used to calculate the zero-shear viscosity of PVME/PS mixtures. In this paper, the spinodals and binodals are calculated with a method not requiring the derivatives of Gibbs energy developed by Horst and Wolf [54,55] for PVME/PS mixtures under shear. A partly quantitative comparison between the theoretical calculations and Higgins'

* Corresponding author. Tel.: +86-431-5262206; fax: +86-431-3685653.

E-mail address: ljan@ns.ciac.jl.cn (L. An).

[1] Present address: Physical Chemistry I, University of Dortmund, Otto-Hahn Str. 6, 44227 Dortmund, Germany.

[2] Present address: Department of Chemistry, University of Toronto, Toronto, Ont., Canada M5S 3H6.

0032-3861/02/$ - see front matter
PII: S0032-3861(02)00227-6

experimental data [40,41] is made. Also the shear rate influence on cloud point temperature and the combining effects of pressure and shear on spinodals are discussed at a certain composition.

2. Theoretical part

From the statistical thermodynamics of lattice fluid model, it is known that the Gibbs energy is expressed as [50]

$$G = -kT \ln Z \tag{1}$$

where

$$Z = \sum_{N_0=0}^{\infty} \Omega \exp[-(E + PV)/kT] \tag{2}$$

Ω is the number of configurations available to a system of N r-mers and N_0 empty sites, E is the total energy of system, V, the system volume, T, the temperature, P, the pressure, and k is the Boltzmann's constant.

For the flowing fluid, E can be expressed as the following equation

$$E = E_0 + E_s \tag{3}$$

where E_0 is the lattice energy and E_s is the energy [32] that a system can store in the stationary state while it flows, and

$$E_s = VJ_e^0(\eta\dot{\gamma})^2|\eta\dot{\gamma}|^{-2d^*} \tag{4}$$

J_e^0 is the steady-state shear compliance, η, the viscosity of the homogeneous system at a shear rate $\dot{\gamma}$, and $d^* = -(\partial \ln \eta)/(\partial \ln \dot{\gamma})$. Substituting Eqs. (2)–(4) into Eq. (1), we have:

$$G \approx -kT \ln \Omega + E_0 + PV\left[1 + J_e^0(\eta\dot{\gamma})^2|\eta\dot{\gamma}|^{-2d^*}/P\right] \tag{5}$$

In the framework of SLLF model, we can derive the reduced Gibbs energy ($\tilde{G}$) and the equation of state for pure fluids as follows

$$\tilde{G}_i = \frac{G_i}{r_i^0 N_i \varepsilon_{ii}^*} = -\tilde{\rho}_i + \tilde{P}_i\tilde{v}_i\xi_i + \tilde{T}_i\left[(\tilde{v}_i - 1)\ln(1 - \tilde{\rho}_i) + \frac{1}{r_i^0}\ln\left(\frac{\tilde{\rho}_i}{\omega_i^0}\right)\right] \tag{6}$$

$$\tilde{\rho}_i^2 + \tilde{P}_i\xi_i + \tilde{T}_i\left[\ln(1 - \tilde{\rho}_i) + \left(1 - \frac{1}{r_i^0}\right)\tilde{\rho}_i\right] = 0 \tag{7}$$

for fluid mixtures

$$\tilde{G} = \frac{G}{rN\varepsilon^*} = -\tilde{\rho} + \tilde{P}\tilde{v}\xi + \tilde{T}\left[(\tilde{v} - 1)\ln(1 - \tilde{\rho}) + \frac{1}{r}\ln\tilde{\rho} + \sum_i \frac{\phi_i}{r_i}\ln\left(\frac{\phi_i}{\omega_i}\right)\right] \tag{8}$$

$$\tilde{\rho}^2 + \tilde{P}\xi + \tilde{T}\left[\ln(1 - \tilde{\rho}) + \left(1 - \frac{1}{r}\right)\tilde{\rho}\right] = 0 \tag{9}$$

where

$$\tilde{X}_i = X/X_i^*, \qquad \tilde{X} = X/X^* \tag{10}$$

$X = T, P, v$ on the left-hand side and $X = T, P, V$ on the right-hand side, and

$$1/v^* = \phi_1/v_1^* + \phi_2/v_2^* \qquad \left(V_i^* = r_i^0 N_i v_i^* \text{ and } V^* = rNv^*\right) \tag{11}$$

$$\varepsilon^* = \sum_{i=1}^{n} \phi_i^2\varepsilon_{ii}^* + \sum_{i\neq j}\phi_i\phi_j\varepsilon_{12}^* \tag{12}$$

$$\xi_i = 1 + J_{e,i}^0(\eta_i\dot{\gamma})^2|\eta_i\dot{\gamma}|^{-2d_i^*}/P \tag{13}$$

$$\xi = 1 + \left\langle J_e^0\right\rangle(\langle\eta\rangle\dot{\gamma})^2|\langle\eta\rangle\dot{\gamma}|^{-2d^*}/P \tag{14}$$

$$1/r = \sum_i \phi_i/r_i \tag{15}$$

$\langle\eta\rangle$ and η_i are the viscosities of mixtures and component i at a given shear rate $\dot{\gamma}$, respectively; $\langle J_e^0\rangle$ and $J_{e,i}^0$ are the steady-state shear compliances of mixtures and component i, respectively; the other parameters in the equation of state and Gibbs energy are defined in Refs. [50–52]. When the shear rate is equal to zero, ξ and ξ_i are unity and the above theory reduces to the original SLLF model.

The mixing Gibbs energy increment per mer for the fluid mixtures is defined as

$$\Delta g = g - \sum_i \phi_i g_i \tag{16}$$

where

$$g = \frac{G}{rN} = \varepsilon^*\tilde{G} \tag{17}$$

$$g_i = \frac{G_i}{r_i^0 N_i} = \varepsilon_{ii}^*\left\{-\tilde{\rho}_i + \tilde{P}_i\tilde{v}_i\xi_i + \tilde{T}_i \times\left[(\tilde{v}_i - 1)\ln(1 - \tilde{\rho}_i) + \frac{1}{r_i^0}\ln\frac{\tilde{\rho}_i}{\omega_i^0}\right]\right\} \tag{18}$$

For the binary mixtures with specific interaction, Sanchez and Balazs [56] have generalized the lattice fluid model by considering the specific interaction between the two components. It is easy to develop the generalized lattice fluid model for polymer blends under shear. In this calculation, the volumes of per mer (per lattice) of pure components and mixture are considered to be the same, i.e. $v_1^* = v_2^* = v^* = v_{PVME}^*$.

3. Rheological background

Viscosity calculation. In this work, $\langle\eta\rangle$ and η_i $(i = 1, 2)$ are calculated by means of the Graessley theory [43,57], i.e.

$$\eta/\eta_0 = g^{1.5}(\theta)h(\theta) \tag{19}$$

$$\theta = (\eta/\eta_0)(\dot{\gamma}\tau_0/2) \tag{20}$$

$$g(\theta) = (2/\pi)[\text{arccot}\ \theta + \theta/(1 + \theta^2)] \tag{21}$$

$$h(\theta) = (2/\pi)[\text{arccot}\ \theta + \theta(1 - \theta^2)/(1 + \theta^2)^2] \tag{22}$$

where $\eta = \langle\eta\rangle$ or η_i; η_0 is the viscosity at a zero-shear rate and $\eta_0 = \langle\eta_0\rangle$ or η_{0i}; $\langle\eta_0\rangle$ and η_{0i} correspond to those of mixtures and component i; τ_0 is the characteristic viscometric relaxation time and $\tau_0 = \langle\tau_0\rangle$ or τ_{0i}; $\langle\tau_0\rangle$ and τ_{0i} correspond to those of mixtures and component i, respectively.

For pure components at a given temperature, the zero-shear viscosity can be obtained from the following relation

$$\eta_{0i}(T_{0i}) = K_i(T_{0i})M_i^{3.4} \tag{23}$$

where $K_i(T_{0i})$ is a constant at a given temperature, M_i is the molecular weight of component i in the unit kg/mol. The temperature and pressure dependences on viscosity in pure components can be described by the following Arrhenius relation [58]

$$\eta_{0i}(T) = \eta_{0i}(T_{0i})\exp\left[\frac{E_i^{\neq}}{R}\left(\frac{1}{T} - \frac{1}{T_{0i}}\right)\right]\exp\left(\frac{PV_i^{\neq}}{RT}\right) \tag{24}$$

where $E_i^{\neq}$ and $V_i^{\neq}$ are the activation energy and the volume of component i, respectively, and R is the gas constant.

Combining rules. For the PVME/PS mixtures, the zero-shear viscosity can be calculated by means of the following expression, which has been proved to be valid by Wolf et al. [53]

$$\ln\langle\eta_0\rangle = \phi_1 \ln \eta_{01} + \phi_2 \ln \eta_{02} + \ln(\eta_{02}/\eta_{01})(\gamma\phi_1\phi_2)/(1 + \gamma\phi_2) \tag{25}$$

where $\gamma = -0.35$ is a geometric factor, measuring the difference between volume and surface fractions.

In the subsequent calculation, the characteristic viscometric relaxation time of the pure component was set to their Rouse relaxation time τ_R [43,59]

$$\tau_{0i} = \tau_R = 6\eta_{0i}M_i/\left(\pi^2\rho_i RT\right) \tag{26}$$

where ρ_i is the density of component i when the temperature is T. According to the following equation [60]

$$J_e^0 = \tau_0/\eta_0 \tag{27}$$

we can obtain the steady-state shear compliance of pure component i:

$$J_{e,i}^0 = 6M_i/\left(\pi^2\rho_i RT\right) \tag{28}$$

Substituting Eq. (27) into Eq. (25), it is given

$$\ln\langle J_e^0\rangle = \phi_1 \ln J_{e,1}^0 + \phi_2 \ln J_{e,2}^0 + \ln\left(J_{e,2}^0/J_{e,1}^0\right)(\gamma\phi_1\phi_2)/(1 + \gamma\phi_2) + \ln\langle\tau_0\rangle - [\phi_1 \ln \tau_{01} + \phi_2 \ln \tau_{02} + \ln(\tau_{02}/\tau_{01}) \times (\gamma\phi_1\phi_2)/(1 + \gamma\phi_2)] \tag{29}$$

From Eq. (28), it is obvious

$$F(\phi_1, \phi_2, T) = \ln\langle\tau_0\rangle - [\phi_1 \ln \tau_{01} + \phi_2 \ln \tau_{02} + \ln(\tau_{02}/\tau_{01}) \times (\gamma\phi_1\phi_2)/(1 + \gamma\phi_2)] \tag{30}$$

In order to keep the completeness of the combining rule on compliance, let

$$F(\phi_1, \phi_2, T) = \phi_1\phi_2 f(T) \tag{31}$$

we have

$$\ln\langle J_e^0\rangle = \phi_1 \ln J_{e,1}^0 + \phi_2 \ln J_{e,2}^0 + \phi_1\phi_2\left[\ln\left(J_{e,2}^0/J_{e,1}^0\right)\gamma/(1 + \gamma\phi_2) + f(T)\right] \tag{32}$$

where $f(T)$ is a function which is dependent on temperature.

Rheological data. For pure PS, the parameter (K_2) in Eq. (23) at $T_{02} = 217$ °C and the active energy $(E_2^{\neq})$ in Eq. (24) are obtained from the experimental data of Fox and Flory [61]. The corresponding parameters of pure PVME, K_1 $(T_{01} = 95$ °C) and $E_1^{\neq}$, are calculated from Higgins' experimental value [40] and are given by Wolf et al. [53]. The above rheological data are listed in Table 1. From Ref. [62], the active volume parameter of pure PS, $V_2^{\neq}$, in Eq. (24) is estimated to be about 10^{-4} m^3/mol. The parameter, $V_1^{\neq}$, in Eq. (24) has not been found from the past reports for PVME. For convenience, let $V_1^{\neq} = V_2^{\neq} = 10^{-4}$ m^3/mol.

4. Results and discussion

From the previous work [63], the SLLF model gave a good description of the phase diagram of PVME/PS systems. Meanwhile, we found that it is enough to calculate the cloud point curves with LCST for the PVME/PS mixtures. In the calculation, ε_{12}^* is not considered as a function of shear rate and the adjustable energy parameter, ε_{12}^*/k, is equal to 696.475 K. The scaling parameters and the

Table 1
Rheological data for PVME and PS [53,61]

	$K(T_0)$ (Pas/(kg/mol)$^{3.4}$)	T_0 (K)	$E^{\neq}$ (J/mol)
PVME	4.24×10^{-5}	368.15	69 676
PS	6.80×10^{-5}	490.15	143 957

Table 2
Scaling parameters of PVME and PS [57,65]

	T_i^* (K)	P_i^* (MPa)	ρ_i^* (g/cm^3)
PVME	657	362.7	1.100
PS	735	405.8[a]	1.105

[a] In this calculation, we considered that the close-packed volume of PS and mixtures are equal to that of PVME, i.e. $P^*_{PS} = T^*_{PS}P^*_{PVME}/T^*_{PVME}$.

molecular parameters of pure PVME and PS are listed in Tables 2 and 3, respectively.

Effects of shear on equation of state. It is known that the shear effects on the equation of state and Gibbs energy mainly come from the factors, ξ_i $(i = 1, 2)$ and ξ, in the pure components and mixtures from the previous derivations. The influences of temperature and shear rate on ξ_i are, respectively, shown in Figs. 1 and 2. From Figs. 1 and 2, we can see that ξ_i is approximately equal to 1.0 in the ranges of temperatures and shear rates calculated for pure PS and there is a small shift at lower temperature and higher shear rate for pure PVME but the difference is less than 4.0%. Therefore, it stands to reason that the scaling parameters [56,64] of pure components under zero-shear rate can be used in this calculation.

Fig. 3 shows ξ of the PVME/PS mixture as a function of composition at different temperatures. A maximum can be found from the ξ–ϕ curve. From the calculated results of ξ, it is known that the effect of shear on the equation of state of PVME/PS mixtures cannot be omitted. In addition, we found that the temperature and composition of ξ_{max} exactly correspond to those of the miscibility gap induced by shear in the spinodals. On the basis of the earlier discussion, it can be concluded that the shear-induced demixing and mixing in PVME/PS system originate mainly from the effects of shear on the Gibbs energy and the equation of state of mixtures.

Shear influence on phase diagram. The calculated spinodals and binodals of the PVME/PS mixtures are shown in Figs. 4 and 5 for the zero-shear and $\dot{\gamma} = 1.14\ s^{-1}$, respectively. From the experimental data [40,41], it is obvious that the system PVME/PS (70/30 at weight ratio) phase separated at ~79 °C (the quiescent cloud point temperature was 93.8 °C) by shear-induced demixing. With increasing temperature, a clear point appeared at ~95 °C and it means that the sample remixed. Finally, at ~103 °C, the PVME/PS mixture phase separated again. Therefore, there were two cloud point temperatures, one at 79 °C corresponding to shear-induced demixing and another at 103 °C corresponding to shear-induced mixing. Furthermore, it is seen that the calculated binodals almost coincide with the

Table 3
Molecular parameters of PVME and PS

	M_i (kg/mol)	r_i^0
PVME89	89	5377
PS330	330	19 848

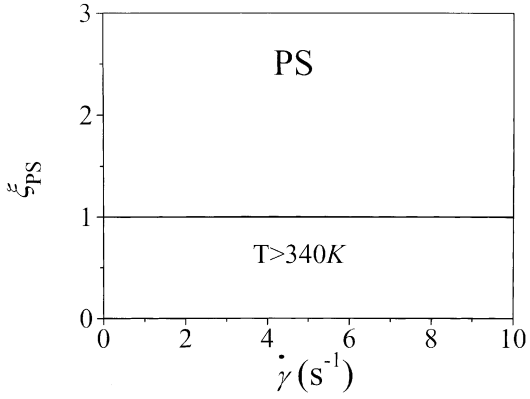

Fig. 1. The shear rate dependence of ξ-parameters of pure PS. The used temperature is higher than the minimum temperature of cloud points (about 340 K).

experimental cloud points and clear point obtained by Higgins et al. [40]. In the spinodals of Fig. 5, a thin, long and banana miscibility gap induced by shear is seen below the miscibility gap with LCST. Owing to the banana miscibility gap, the lower temperature by shear-induced demixing and higher temperature by shear-induced mixing can be observed in the PVME/PS mixture with a certain composition (PVME/PS = 70/30 at weight ratio). The conclusion is identical with the results calculated by means of the model system [42–44].

From the calculated binodals under shear (Fig. 5), we can see the stable (solid line) and metastable (dotted lines) binodals, and the binodal coalescence of upper and lower miscibility gaps is observed. In addition, the metastable binodals disappear when one branch of them intrudes into the spinodal. Meanwhile, the three points of the three-phase equilibrium are found at about $T = 376.24$ K. The phenomenon can be explained from the thermodynamics [65].

As shown in Figs. 3 and 5, though the increment of the parameter ξ resulted in the stored energy is lower (<10%), it is enough to induce a banana miscibility gap below the miscibility gap with LCST and to make a peculiar phenomenon for the phase separation behavior of the system PVME/PS. The zone of additional heterogeneity created

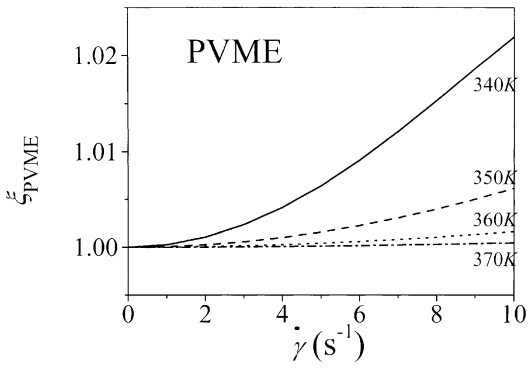

Fig. 2. The temperature and shear rate dependence of ξ-parameters of pure PVME. The different lines indicate the different temperatures.

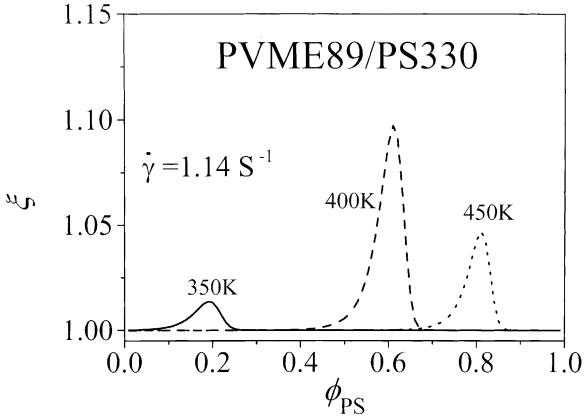

Fig. 3. The ξ-parameter of PVME/PS blend is as a function of concentration of PS at different temperatures. The shear rate is 1.14 s^{-1} and the different lines indicate different temperatures.

by shear emerges from the equilibrium two-phase region and centers around the curve of temperature dependence on composition, at which the stored energy becomes maximum for the shear rate given, also shown in Fig. 5. The situation presented is very similar to that reported by Katsaros et al. [10] for mixtures of two polymers differing considerably in chain length. A temperature interval of homogeneity separating two miscibility gaps has been observed for a polymer concentration fixed.

However, the different data of the phase diagrams for the systems PS/PVME have been presented by Madbouly et al. [66]. Madbouly et al. showed that the cloud point temperature decreased and then increased with increasing shear rate. The theoretical explanation is in progress in our group.

Shear rate dependence on cloud point shift. For a PVME/PS = 70/30 mixture (at weight ratio), the difference between the cloud point temperature of shear-induced demixing and mixing (T_c^d and T_c^m) and the quiescent cloud point temperature (T_c) was calculated at different shear rate, respectively. The theoretical curve and the experimental results [40,41]

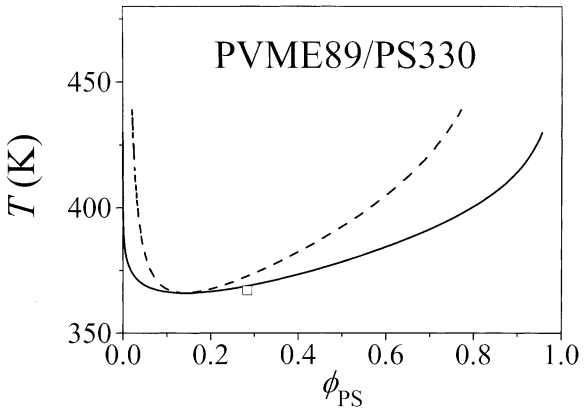

Fig. 4. The calculated quiescent phase diagram together with the experimental cloud point of PVME89/PS330. The dashed line is calculated spinodal and the solid line is corresponding to binodal. The open symbol is the experimental cloud point [40].

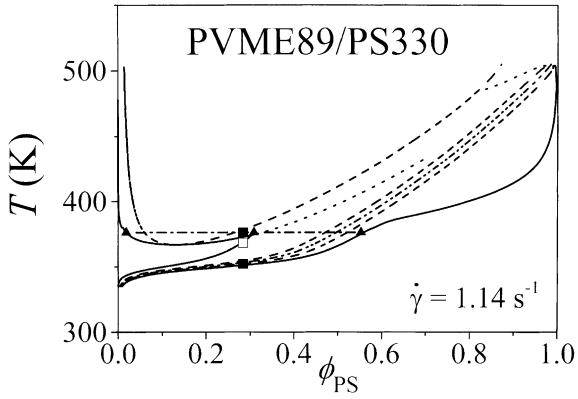

Fig. 5. The spinodal, metastable and stable binodals at shear rate 1.14 s^{-1}. Solid squares: experimental cloud points [40]; open square: experimental clear point [40]; Solid up-triangles: three-phase points. Dashed lines: calculated spinodals; dotted lines: calculated metastable binodals; solid lines: calculated stable binodals; dash-dotted line: the straight line of the three-phase points; dash-dot-dotted line: dependence of temperature on composition at which the stored energy becomes maximum for the shear rate given.

are shown in Fig. 6. According to the calculated results, the absolute ratio of the cloud point temperature difference ($\Delta T_c^d = T_c^d - T_c$) to T_c decreases with the increase of shear rate and the ratio between ΔT_c^m ($= T_c^m - T_c$) and T_c increases with the increase of shear rate. The theoretical results describe the Higgins experimental data partly. However, the minimum of $(T_c^d - T_c)/T_c$ and the maximum of $(T_c^m - T_c)/T_c$ with the increase of shear rate suggested by Higgins et al. [40,41] were not found in our calculation. The $\Delta T_c/T_c$–P diagram of shear-induced demixing at very low shear rates is shown at the up-left of Fig. 6. The $\Delta T_c/T_c$ decrease quickly when the shear rate is very low and then increases slowly with the increase of shear rate.

Prediction of the combining effects of pressure and shear on spinodal shift. In order to evaluate the dependence of phase diagram on pressure, the interaction energy ε_{12}^* should be considered as a linear function of pressure according to our previous work [32,67], i.e.

$$\varepsilon_{12}^* = \varepsilon_{12}^*(P = P_0) + (P - P_0)v_{12}^* \tag{33}$$

Because of lack of experimental phase diagrams of PVME/PS at different pressures, it is hard to give the concrete relationship between interaction energy ε_{12}^* and pressure. In this work, we assumed v_{12}^*/k to be -0.0018 K/bar. [67][3] The $\Delta T_c/T_c$–P phase diagrams are shown in Fig. 7, where the dashed line is corresponding to the shear-induced mixing at different pressures and the dotted line is the shear-induced demixing. The weight fraction of PS is 0.3. From Fig. 7, we can see that the shear-induced mixing becomes inconspicuous with the increase of pressure and the shear-induced demixing becomes more and more visible.

Prediction of shear effect on Flory–Huggins interaction parameter. On the basis of the Flory–Huggins lattice model

[3] For the system PVME/d-PS, v_{12}^*/k is 0.009 K/bar. Here, we defined v_{12}^*/k as 0.0018 K/bar according to the calculated P–T phase diagrams [66].

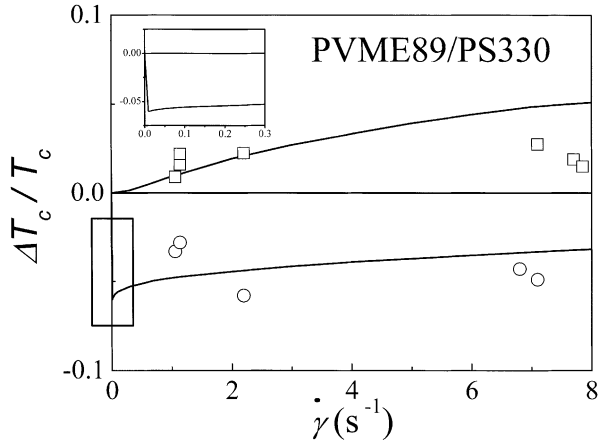

Fig. 6. The cloud point shift as a function of the shear rate for PVME/PS = 70:30 (weight fraction). Open squares: experimental positive shift of cloud points [40]; open circles: experimental negative shift of cloud points [40]; solid lines: the calculated shift of cloud points from metastable and stable binodals. The zoomed area in the frame is shown in the upper left of this figure.

[68], the Flory–Huggins interaction parameter γ can be expressed as

$$\gamma = \frac{\frac{\Delta G_M^{FH}}{kTV} - \left(\frac{\varphi_1}{V_1}\ln\varphi_1 + \frac{\varphi_2}{V_2}\ln\varphi_2\right)}{\varphi_1\varphi_2} \tag{34}$$

where φ_i is the volume fraction of component i, and ΔG_M^{FH} is the Gibbs energy of mixing in the FH theory. To calculate the Flory–Huggins interaction parameter, we use two assumptions as we have done in our previous papers [69], then Eq. (34) becomes:

$$\begin{aligned}\gamma = \frac{1}{(v^*\tilde{v})\phi_1\phi_2}\Bigg\{ & \frac{-\tilde{\rho} + \tilde{P}\tilde{v}\xi}{\tilde{T}} - \Bigg[\phi_1\frac{-\tilde{\rho}_1 + \tilde{P}_1\tilde{v}_1\xi_1}{\tilde{T}_1} \\ & + \phi_2\frac{-\tilde{\rho}_2 + \tilde{P}_2\tilde{v}_2\xi_2}{\tilde{T}_2}\Bigg] + (\tilde{v}-1)\ln(1-\tilde{\rho}) + \frac{1}{r}\ln\tilde{\rho} \\ & - \Bigg[\phi_1\left((\tilde{v}_1-1)\ln(1-\tilde{\rho}_1) + \frac{1}{r_1^0}\ln\tilde{\rho}_1\right) \\ & + \phi_2\left((\tilde{v}_2-1)\ln(1-\tilde{\rho}_2) + \frac{1}{r_2^0}\ln\tilde{\rho}_2\right)\Bigg] \\ & + \phi_1\left(\frac{1}{r_1^0}\ln\omega_1^0 - \frac{1}{r_1}\ln\omega_1\right) \\ & + \phi_2\left(\frac{1}{r_2^0}\ln\omega_2^0 - \frac{1}{r_2}\ln\omega_2\right)\Bigg\}\end{aligned} \tag{35}$$

Figs. 8 and 9 show the concentration and temperature dependences of Flory–Huggins interaction parameters at zero-shear rate and 1.14 s^{-1}. The dotted and solid lines represent the quiescent Flory–Huggins interaction parameters and the sheared ones, respectively. It can be found that there is an extremum with the increase of concentration of PS at different temperatures (Fig. 8) and there are also extrema with the increase of the reciprocal of temperature at $\phi_{PS} = 0.5$ and 0.9 in the temperature range of our interest. Furthermore, the Flory–Huggins interaction parameter is almost linear dependent on the inverse of temperature when the volume fraction of PS is 0.1 (Fig. 9). The concentrations and temperatures of those extrema are still corresponding to those of shear-induced miscibility gap of the spinodals.

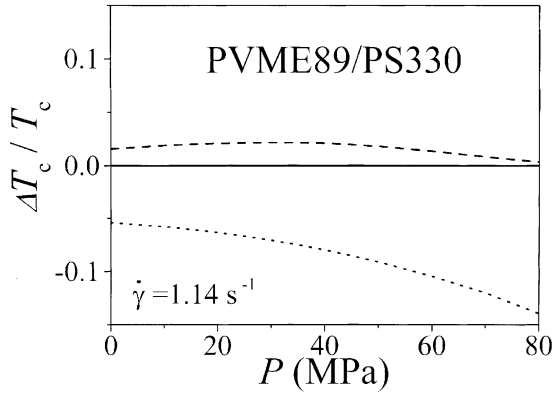

Fig. 7. The cloud point shift calculated as a function of pressure for PVME/PS = 70:30 (weight fraction). Dashed line: the shift of shear-induced mixing; dotted line: the shift of shear-induced demixing.

5. Conclusions

From the above derivations and calculated results, the main conclusions of this paper are summarized as follows:

1. The shear influence on the Gibbs energy and equation of

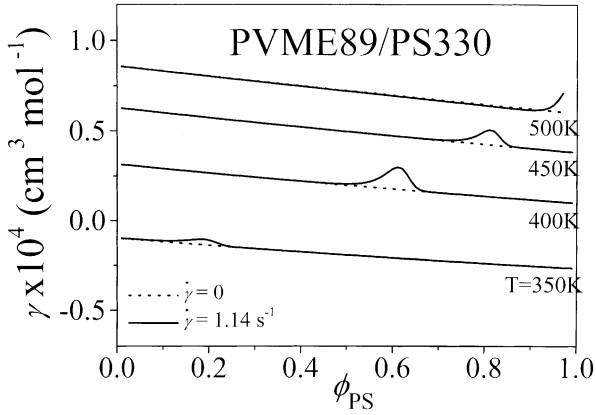

Fig. 8. Concentration dependence of Flory–Huggins interaction parameters of PVME/PS at zero-shear and 1.14 s^{-1}. Dotted lines: Flory–Huggins interaction parameters at zero-shear; solid lines: those at 1.14 s^{-1} shear rate.

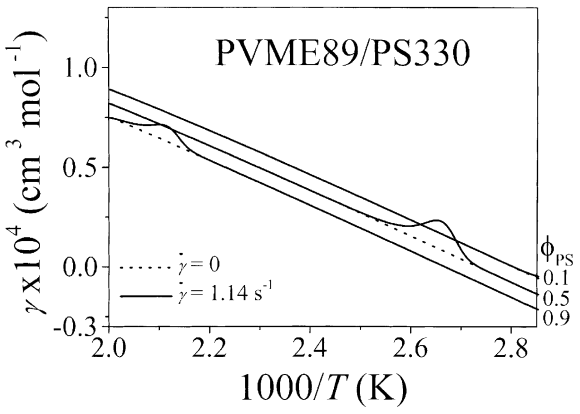

Fig. 9. Temperature dependence of Flory–Huggins interaction parameters of PVME/PS at zero-shear and 1.14 s^{-1}. Dotted lines: Flory–Huggins interaction parameters at zero-shear; solid lines: those at 1.14 s^{-1} shear rate.

state is embodied only by ξ. With the increase of the concentration of PS, there are extrema, and the concentrations and temperatures of those extrema are corresponding to those of shear-induced miscibility gap of the spinodals exactly, which is similar to the effect of Flory–Huggins interaction parameters.

2. There are three points of the three-phase equilibrium at about $T = 376.24$ K on stable binodal.
3. The shear-induced mixing becomes inconspicuous and the shear-induced demixing becomes conspicuous with the increase of pressure.

Acknowledgements

This work is supported by the National Natural Science Foundation of China for the National Science Fund for Distinguished Young Scholars of China (No. 59825113), the General Program (29704008, 20074037 and 50073023) and the Special Fund (20023003 and 50027001), the Special Funds for Major State Basic Research Projects (No. G1999064800), and the Scientific and Technological Department of Jilin Province.

References

[1] Mazich KA, Carr SH. J Appl Phys 1983;54:5511.
[2] Wolf BA. Macromolecules 1984;17:615.
[3] Ueda H, Karasz FE. Macromolecules 1985;18:2719.
[4] Katsaros JD, Malone MF, Winter HH. Polym Bull 1986;16:83.
[5] Hashimoto T, Takebe T, Suehiro S. Polym J 1986;18:129.
[6] Tirrell M. Fluid Phase Equilib 1986;30:367.
[7] Lyngaae-Jørgensen J, Søndergaard K. Polym Engng Sci 1987;27:344, see also page 351.
[8] Rector LP, Mazich KA, Carr SH. J Macromol Sci, Phys 1988;B27:421.
[9] Larbi FBC, Malone MF, Winter HH, Halary JL, Leviet MH, Monnerie L. Macromolecules 1988;21:3532.
[10] Katsaros JD, Malone MF, Winter HH. Polym Engng Sci 1989;29:1434.
[11] Vshivkov SA, Pastukhova LA, Titov RV. Polym Sci USSR (Engl Transl) 1989;31:1541.
[12] Nakatani AI, Kim H, Takahashi Y, Han CC. Polym Commun 1989;30:143.
[13] Hindawi I, Higgins JS, Galambos AF, Weiss RA. Macromolecules 1990;23:670.
[14] Nakatani AI, Kim H, Takahashi Y, Matsushita Y, Takano A, Bauer BJ, Han CC. J Chem Phys 1990;93:795.
[15] Kammer HW, Kummerloewe C, Kressler J, Melior JP. Polymer 1991;32:1488.
[16] Ishikawa K, Kawahara S, Akiyama S. Polym Networks Blends 1991;1:1.
[17] Douglas JF. Macromolecules 1992;25:1468.
[18] Hindawi IA, Higgins JS, Weiss RA. Polymer 1992;33:2522.
[19] Jinnai H, Hasegawa H, Hashimoto T, Han CC. Macromolecules 1992;25:6078.
[20] Larson RG. Rheolog Acta 1992;31:497.
[21] Mani S, Malone MF, Winter HH. Macromolecules 1992;25:5671.
[22] Tomura H, Saito H, Inoue T. Macromolecules 1992;25:1611.
[23] Muniz EC, Nunes SP, Wolf BA. Makromol Chem Phys 1994;195:1257.
[24] Soontaranum W, Higgins JS, Paoathanasiou TD. J Non-Newtonian Fluid Mech 1996;67:191.
[25] Soontaranun W, Higgins JS, Papathanasiou TD. Fluid Phase Equilib 1996;121:273.
[26] Hobbie EK, Nakatani AI, Yajima H, Douglas JF, Han CC. Phys Rev E 1996;53:R4322.
[27] Fernandez ML, Higgins JS, Richardson SM. J Mater Proc Technol 1996;56:807.
[28] Nakatani AI, Sung L, Hobbie EK, Han CC. Phys Rev Lett 1997;79:4693.
[29] Clarke N, Mcleish TCB, Pavawongsak S, Higgins JS. Macromolecules 1997;30:4459.
[30] Yu J-W, Douglas JF, Hobbie EK, Kim S, Han CC. Phys Rev Lett 1997;78:2664.
[31] Krause C, Horst R, Wolf BA. Macromolecules 1997;30:890.
[32] An L, Wolf BA. Macromolecules 1998;31:4621.
[33] Horst R, Wolf BA. Polym Bull 1998;40:353.
[34] Wolf BA. J Chem Phys 1999;110:7542.
[35] Chopra D, Haynes C, Hatzikiriakos SG, Vlassopoilos D. J Non-Newtonian Fluid Mech 1999;82:367.
[36] Hinrichs A, Wolf BA. Macromol Chem Phys 1999;200:368.
[37] Lazo NDB, Scott CE. Polymer 1999;40:5469.
[38] Furgiuele N, Lebovitz AH, Khait K, Torkelson JM. Macromolecules 2000;33:225.
[39] An L, Hinrichs A, Horst R, Krause C, Wolf BA. Macromol Symp 2000;149:75.
[40] Fernandez ML, Higgins JS, Horst R, Wolf BA. Polymer 1995;36:149.
[41] Fernandez ML, Higgins JS, Richardson SM. Trans Inst Chem Engng 1993;71A:239.
[42] Horst R, Wolf BA. Macromolecules 1991;24:2236.
[43] Horst R, Wolf BA. Macromolecules 1992;25:5291.
[44] Horst R, Wolf BA. Macromolecules 1993;26:5676.
[45] Flory PJ. J Chem Phys 1941;9:660.
[46] Flory PJ. J Chem Phys 1942;10:51.
[47] Huggins ML. J Chem Phys 1941;9:440.
[48] Huggins ML. Ann NY Acad Sci 1942;43:1.
[49] Schuch H. Rheol Acta 1988;27:384.
[50] Sanchez IC, Lacombe RH. J Phys Chem 1976;80:2352.
[51] Lacombe RH, Sanchez IC. J Phys Chem 1976;80:2568.
[52] Sanchez IC, Lacombe RH. Macromolecules 1978;11:1145.
[53] Kapnistos M, Hinrichs A, Vlassopoilos D, Anastasiadis SH, Stammer A, Wolf BA. Macromolecules 1996;29:7155.
[54] Horst R. Macromol Theor Simul 1995;4:449.
[55] Horst R, Wolf BA. J Chem Phys 1995;103:3782.
[56] Sanchez IC, Balazs AC. Macromolecules 1989;22:2325.
[57] Graessley WW. Adv Polym Sci 1974;16:1.

[58] Wolf BA, Jend R. Macromolecules 1979;12:732.
[59] Rouse PE. J Chem Phys 1953;21:1272.
[60] Laun HM. Prog Colloid Polym Sci 1987;75:11.
[61] Fox Jr TG, Flory PJ. J Am Chem Soc 1948;70:2384.
[62] Meister BJ. Encyclopedia of polymer science and engineering. 2nd ed., vol. 16. p. 127, 1989.
[63] An L, Wolf BA. J Macromol Sci, Pure Appl Chem 1997;A34:1629.
[64] Sanchez IC, Lacombe RH. J Polym Sci, Polym Lett Ed 1977;15:71.
[65] Šolc K, Koningsveld R. J Phys Chem 1992;96:4056.
[66] Madbouly S, Ohmomo M, Ougizawa T, Inoue T. Polymer 1999;40:1465.
[67] An L, Horst R, Wolf BA. J Chem Phys 1997;107:2597.
[68] Flory PJ. Principles of polymer chemistry. Ithaca, NY: Cornell University Press, 1953.
[69] Sun Z, An L, Jiang Z, Ma R, Wu Z. J Macromol Sci, Phys 1999;B38:67.